Comparison of Post stack Seismic Inversion Methods:A case study from Blackfoot Field, Canada

S.P. Maurya[1] and P. Sarkar[1]

[1]Department of Earth Sciences, Indian Institute of Technology, Bombay, Powai, Mumbai-400076, India.
Email: spm.bhu@gmail.com

ABSTRACT: Seismic Inversion methods have been routinely used for estimating attributes like P-impedance, S-impedance, density, ratio of P-wave and S-wave velocity and elastic impedances from seismic and well log data. These attributes help to understand lithology and fluid contents in the subsurface. The objective of this research is to use several standard seismic post-stack inversion methods for reservoir characterization and compare their results. Model-based (MBI), Colored (CI), Sparse-spike (SSI), and Band-limited (BLI) inversions are applied to the post-stack seismic data from the Blackfoot field, Alberta, Canada. In each case the data is inverted into P-impedance and density volume. The final stacked section shows high-resolution images within the time-depth ranges of 300 to 1300ms. All inversions show mutually consistent results with low-impedances within the target hydrocarbon sand within the channel. All post-stack inversion methods produces accurate and reliable results and unequivocally confirm the presence of reservoir in the channel area at 1060-1065ms time. Model based inversion methods shows higher correlation coefficient (0.99) and least RMS Error (778 m/s*g/cc) and hence better for Blackfoot seismic data.

Geostatistical methods-Probabilistic neural network is also employed to estimate the petrophysical (porosity) variations within the sand channel (reservoir) of the Blackfoot field. The Correlation coefficients between the predicted and measured porosities following that the probabilistic neural network show that Sparse spike Inversion when used as an external attribute, is more accurate and produces high-resolution image compared to that estimated with the use of model based and Colored Inversion as an attribute. From the estimates, the predicted logs show correlation of 0.81, 0.84 and 0.86 using neural network algorithm and MBI, CI and LPSSI as external attribute, respectively. Of the four post stack seismic inversion methods used here the probabilistic neural-network method with sparse spike inversion provides a higher correlation coefficient than that estimated for other methods.

Keywords: Model-based inversion, Colored Inversion, Sparse-spike Inversion, Band-limited Impedance inversion, Acoustic Impedance, Elastic Impedance, Seismic Processing etc.

1 INTRODUCTION

Seismic inversion is a procedure that helps extract underlying models of the physical characteristics of rocks and fluids from seismic and well-log data. In the absence of well data, the properties can also be inferred from the inversion of seismic data alone [10]. In oil and gas industry, seismic inversion techniques have been widely used as a tool to locate hydrocarbon-bearing strata in the subsurface [19], [14].

The physical parameters that are of interest to a modeler performing inversion are: Impedance (Z), P-wave (V_P) and S-wave (V_S) velocity and density. Lame parameters which are sensitive towards fluid and saturation in rocks [3] can be derived from inverted models of impedances. The petrophysical parameters like porosity, sand/shale ratio and gas saturation can be estimated with the help of inverted volumes [3].

The seismic inversion techniques can be divided into two broad categories: Pre-stack and Post-stack inversion. The first approach in the seismic inversion is the most commonly used where the effect of the wavelet is removed from the seismic data and a high-resolution image of the subsurface is produced [16]. The second approach in seismic inversion relies on model building from well log, seismic and geological data [4]. This also generates a high-resolution image of the subsurface from which reservoir properties are calculated. A reliable estimate of the reservoir properties is critical in decision-making process

during production phase[21]. This study focuses only post-stack seismic inversion methods.

Further, Geostatistical method is used for better estimate of reservoir properties. Geostatistical methods are routinely followed to predict various geophysical parameters from seismic and log data. These methods use colored inversion, model based inversion and sparse spike derived impedances as external attributes and seismic and well log data as internal attributes for the geostatistical analysis [5]. The inversion methods are implemented on the post-stack seismic data. Figure 1 shows flowchart of seismic inversion methods.

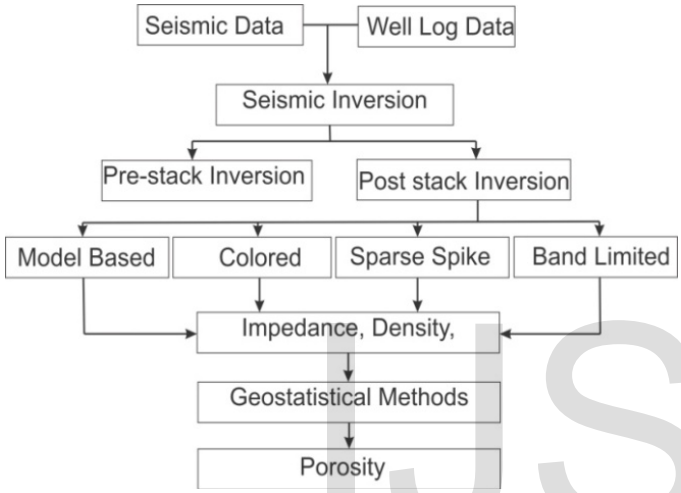

Figure 1: Flow chart of inversion methods used in this study.

Some of the advantages of post-stack inversion methods are mentioned below:

1. The acoustic impedance is a layer property; hence stratigraphic interpretation is easier on impedance data than seismic data.
2. The reduction of wavelet effects, side lobes and tuning enhances the resolution of subsurface layers.
3. The Acoustic impedance can be directly computed and compared to well log measurements that serve as a link to reservoir properties.
4. Porosity can be related to the acoustic impedance. Using geostatistical methods these impedance volume can be transformed to the porosity volume within the reservoir.
5. The Acoustic impedance can be utilized to locate individual reservoir regions.

2 THE STUDY AREA: BLACKFOOT FIELD, CANADA

The Blackfoot field is located south-east of Strathmore, Alberta, Canada. Pan Canadian Petroleum and the CREWES (the Consortium for Research in Elastic-Wave Exploration Seismology) carried out the initial experiments on the data. Filtering and deconvolution was the initial experiments performed on the data [6]. The dataset contains 708 shots into a fixed recording spread of 690 channels. The fold is 140 at the center of the spread [16].

Figure 2: Study area (Blackfoot, Field) shown by red rectangle.

The data was recorded in two overlapping patches: the first patch targeted the clastic Glauconitic channel, and the second one went deeper to study the reef-prone Beaver hill lake carbonates [13]. This paper uses the data from the first patch, which focused on the clastic Glauconitic channel. The details of the processing steps used for the vertical and horizontal component data can be found in [24]. In this study, the conventional (vertical-component) 3D seismic data and thirteen well-log datasets are used for analysis of post stack seismic inversion methods.

3 METHADOLOGY

In the following sections, post stack seismic inversion named, model-based, colored, sparse-spike and band-limited impedance inversion techniques are describebriefly. Geostatistical method is briefly described in the last section of methodology.

3.1 Model-Based Inversion (MBI)

Model Based Inversion is based on the convolutional theory which states that the seismic trace can be generated from the convolution of wavelet with the Earth's reflectivity and addition of noise [15].

$$Seismictrace = Wavelet * Reflectivity + Noise$$

If the noise in the data is uncorrelated with the seismic signal, the trace can be solved for the earth reflectivity function. This is a non-linear equation which can be solved iteratively as follows [12]:

$$Z = V * \rho$$

$$r_i = \frac{Z_{i+1} - Z_i}{Z_{i+1} - Z_i}$$

$$AI_N = AI_1 \exp\left(\sum_{i=1}^{n} r_i\right)$$

These equations are used in practice for recursive inversion with the aim of transforming reflectivity function into acoustic impedance [1]. AI_1 is the acoustic impedance of the first (top) layer and AI_N is the acoustic impedance for the N^{th} layer. r_i is the reflection coefficient of the i^{th} layer. This equation is valid for most of the practical cases where r_j<0.3[1].

The acoustic impedance model of low frequency is obtained by estimating these values over the entire seismic section using kriging interpolation techniques at the wells. Generally, acoustic impedance are not recorded during the acquisition of well log data. These parameters can be estimated directly from the sonic and density log.

The work flow of model based inversion technique is as follows [7]:

1. Calculate the acoustic impedance at well locations using the well log data.
2. Pick horizons in the seismic section to control the interpolation and to provide structural information for model between the wells in the area.
3. Use interpolation along the interpreted seismic horizons and between the well locations to obtain the initial acoustic impedance model.
4. Block the initial impedance using some selected block size.
5. Extract statistical wavelet from the seismic section.
6. Convolve the wavelet with the Earth Reflectivity to obtain synthetic seismic trace. This synthetic trace is different from the observed seismic trace.
7. The Least Squares optimization is performed for minimizing the difference between the real and the modeled reflectivity section. This is achieved by analyzing the misfit between the synthetic trace and the real trace and modifying the block size and the amplitude to reduce the error.
8. Repeat step 7 until the lowest misfit between the real seismic and the synthetic trace is achieved [17].

3.2 Colored Inversion

The colored inversion technique is a process where the spectra of the acoustic impedance derived from log data are used to compute the spectrum of the operator. The phase of this operator is -90^0 which allows its integration with the reflectivity series to generate the impedances[11]. The operator is derived in the following steps: First, the acoustic impedance is calculated and plotted against frequency for all wells in the area (Figure 3). A regression line is fit to the amplitude spectrum of the acoustic impedance to represent the impedance spectrum in the subsurface in the log-log scale. Second, the seismic spectrum is calculated from the seismic traces near the wells (Figure 4). These two spectra are used to calculate the operator spectrum which transforms the seismic spectrum into the average impedance spectrum. Third, the final spectrum is combined with a -90^0 phase shift to create the desired operator in time domain (Figure 5). The operator in frequency domain can be represented as shown in Figure (6). Colored inversion is fast and suitable for application to 3-D datasets [20].

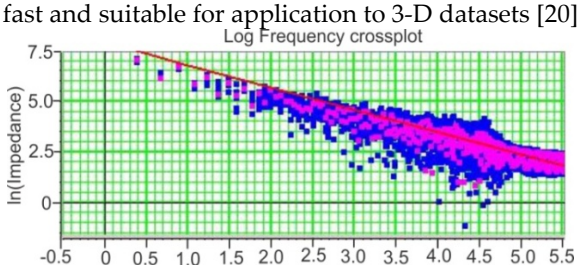

Figure 3:AI from all wells (blue), one selected well (pink) and frequency on log-log scale.

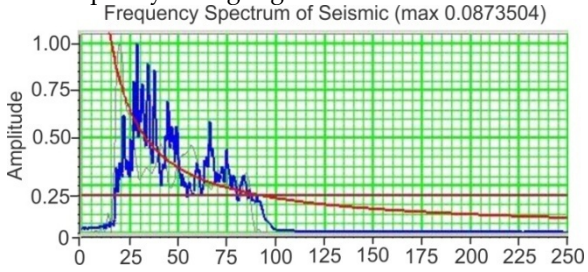

Figure 4: Seismic spectra near the wells (blue). Red line corresponds to the $f^{-\theta}$ AI spectrum derived in figure 2. The operator spectrum (black) is the ratio of these two spectra.

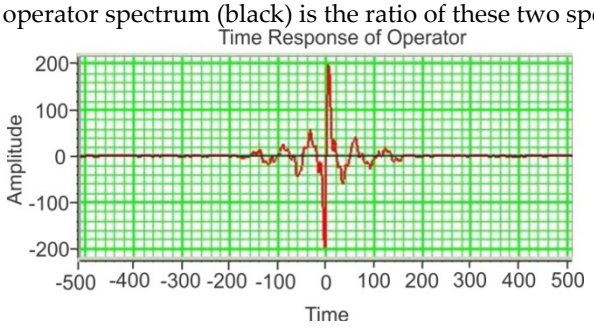

Figure 5: Time response of operator.

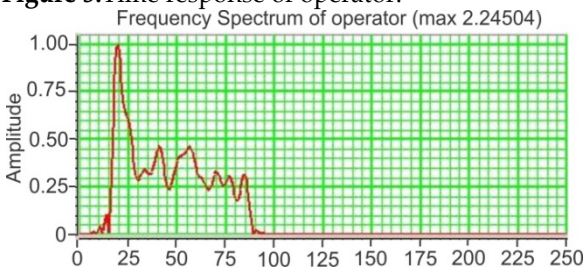

Figure 6: Frequency spectrum of the operator.

3.3 Sparse-Spike Inversion

There are two types of sparse spike inversion techniques used to invert seismic section into impedance. The first one is Linear programming sparse spike and second one is Maximum likelihood sparse spike inversion techniques. These methods are described briefly in the following two subsections.

I. Linear Programming

This algorithm first extracts an estimate of the reflectivity, using programming technique that uses frequency domain constraints to recover the high and frequencies of the seismic spectrum. Then the reflectivity is integrated under the initial model. This creates a sparse reflectivity that produces the best match between derived synthetic and the seismic trace, subject to the constraint that the number of s be a minimum.

It is assumed that the wavelet in the seismic data is known and, in fact, is the current wavelet. This method attempts to recover an impedance model with sparse reflectivity by minimum error between the modeled trace and the seismic trace. The L_1 norm of the reflection is also minimized, which results in an earth model with the number of layers.

II. Maximum Likelihood

This algorithm uses the model to perturb a reflectivity series from the seismic data. It is assumed that the wavelet in the seismic data is known and the current wavelet. For each trace, a sparse reflectivity sequence is estimated by add reflection coefficients one by one until an optimal set has been found. The broadband reflectivity then modified gradually, until the resulting synthetic trace matches the real trace with tolerance level. We can control how far the algorithm may move from the initial guess model to match the real data.

3.4 Band-limited Impedance Inversion

Band-limited impedance inversion (BLI) transforms post stack seismic data into impedance, density and P-wave velocity. The band limited impedance method begins with specifying the relationship between the seismic trace and seismic impedance [7]. Thus, define the normal incidence reflection coefficient as:

$$r_i = \frac{Z_{i+1} - Z_i}{Z_{i+1} - Z_i}$$

Where Z_i is seismic impedance of j^{th} layer and r_i is seismic reflectivity of j^{th} and $(j+1)^{th}$ interface.Solve above equation for impedance $(j+1)^{th}$ layer

$$Z_{j+1} = Z_j\left(1 + \frac{2r_j}{1 - r_j}\right) = Z_j\left(\frac{1 + r_j}{1 - r_j}\right)$$

Impedance of n^{th} layer if we know impedance of 1^{st} layer is:

$$Z_n = Z_1\left(\frac{1 + r_1}{1 - 1}\right)\left(\frac{1 + r_2}{1 - r_2}\right) \ldots \ldots \left(\frac{1 + r_{n-1}}{1 - r_{n-1}}\right)$$

The acoustic impedance for the first layer needs to be estimated from a continuous layer above the target area [18]. In this method, the impedance for the j^{th} layer can thus be calculated as follows:

$$Z_{n+1} = Z_1 \prod_{k=1}^{j}\left(\frac{1 + r_k}{1 - r_k}\right)$$

Divide above equation (4) by impedance of 1st layer that is Z_1 and take the logarithm on both side,

$$\ln\left(\frac{Z_{j+1}}{Z_j}\right) = \sum_{k=1}^{j} \ln\left(\frac{1 + r_k}{1 - r_k}\right) \approx 2\sum_{k=1}^{j} r_k$$

The last step follows from an approximation for ln which is valid only for small r. Now on solving equation (5) for Z_{j+1} we have:

$$Z_{j+1} = Z_1 \exp\left(2\sum_{k=1}^{j} r_k\right)$$

Model the seismic trace as scaled reectivity: $S_K = \frac{2r_k}{\gamma}$, then above equation becomes:

$$Z_{j+1} = Z_1 \exp\left(\gamma\sum_{k=1}^{j} S_K\right)$$

The above equation thus integrates the seismic trace and then exponentiates the result to provide an impedance trace [25], [18].

3.5 Geostatistical Methods

The Geostatistical method use sample points taken at different locations and interpolates in the seismic section where log data are not available. These sample points are measurements of petrophysical parameters in the boreholes [8]. The geostatistics derives a surface using the values from the measured locations to estimate datapoints for each location in between the data points.

Two groups of interpolation techniques are provided by Geostatistics: deterministic and geostatistical [23]. Mathematical function is uses by the Deterministic techniques for interpolation whereas Geostatistics used both statistical and mathematical methods [9].

Geostatistical method is routinely followed to predict various geophysical parameters from seismic and log data. Here we utilize Probabilistic Neural Network to compute porosity volume from seismic data [5]. The procedures followed for the Geostatistical analysis of the data are:

1. The spatial continuity of the well log data is quantified using variograms.
2. A statistical relationship is derived between the log and seismic data at all well locations using cross-validation plots. The Multivariate Regression is linear while the Probabilistic Neural Network displays non-linear relationship.
3. These linear and non-linear relationships are then used to estimate the porosity volume at all locations of the seismic volume.
4. The predicted porosity is evaluated for its reliability.

The result is validated by hiding the wells and predicting the porosity at the same well location using the data from other wells in that area [2]. In this study Probabilistic neural Network is used to transform impedance volume into Porosity volume.

4 RESULTS

4.1 Seismic Inversions

Post-stack seismic inversion operates on NMO-corrected and stacked CMP seismic data. Wavelet extraction is the first step of this inversion. Wavelet is extracted using all thirteen wells available in the study area.

After extracting wavelet,well-log to seismic correlation is the next step which performed for each well individually. The process of correlation is applied as follows:

1. A synthetic trace is generated using well log data and compared it to the seismic trace nearest to the well location;
2. Time stretching and squeezing is applied to the data to align the seismic and well-log reflectors;
3. Correlation coefficient and RMS Error are measured between the seismic and adjusted well-log synthetic traces. Figure

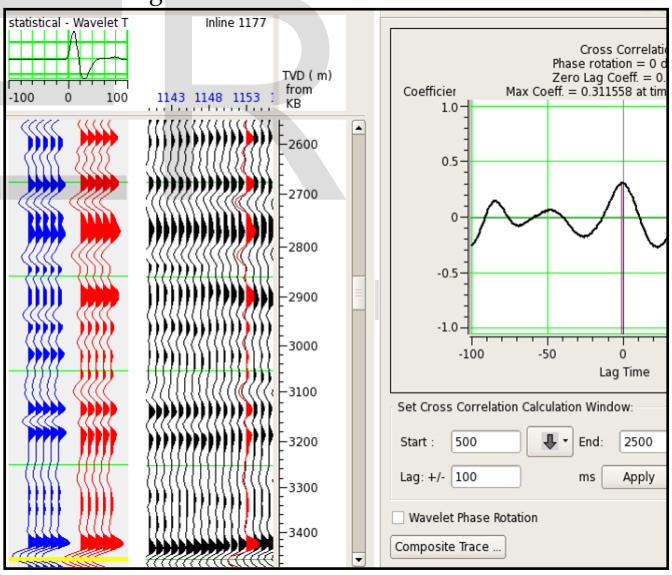

Figure 7: Process of seismic correlation with well log data.

Computation of initial impedance model is the next step of the inversion. This initial impedance model is built by interpolating the acoustic impedance from the well locations into the in-lines and cross-lines. Two interpreted seismic horizons are introduced as guide for the interpolation. To construct the impedance model a 12-Hz

low-pass filter is applied to the model for two reasons. First, the low frequency impedance trend is required in order to recover the low frequencies which are missing from the stacked seismic data. The second is the

impedances above ~12-Hz frequencies should be only obtained from seismic data, and therefore this frequency band should be removed from the well-log data while building the starting impedance model [2].

Next, step is to apply model-based, colored, sparse-spike and band-limited impedance inversion to the real seismic data from the Blackfoot seismic data. This is performed in two steps. First, one composite seismic trace is extracted from seismic data and inverted into impedance. Correlation coefficient (CC) and RMS Errors are estimated. Secondly, If CC and RMS Error are in acceptable range then applied these inversion methods to entire seismic data to invert into impedance and density.

The inversion result at the well location is compared to the original log at well 01-17 are shown in Figure 8. In figure, the red trace shows inverted impedance from the seismic trace, the blue trace shows impedance from well log data and the black trace shows initial guess model.

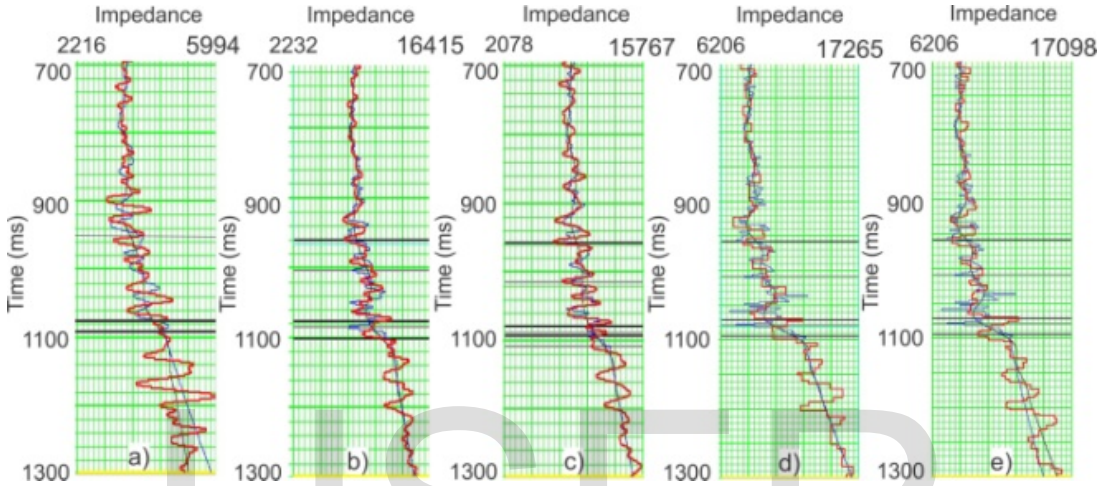

Figure 8: Comparison of Inverted impedance with real impedance from well log data. a) Shows inversion using MBI, b) CI, c) LPSSI, d) MLSSI and e) BLI methods.

Synthetic traces is generated and correlated with the seismic traces for all wells and the differences between them are measured. The match between the synthetic and seismic trace showed good correlations (Figure 9) for most wells. The correlation coefficients are varies from 0.80 to 0.99.

Figure 10 shows comparison of relative error with all boreholes for all inversion methods. The figure shows that the relative error of MLSSI is largest and LPSSI is smallest. The root mean square (RMS) errors are also estimated and it is vary from 500 (m/s)*(g/cc) to 1250 (m/s)*(g/cc).

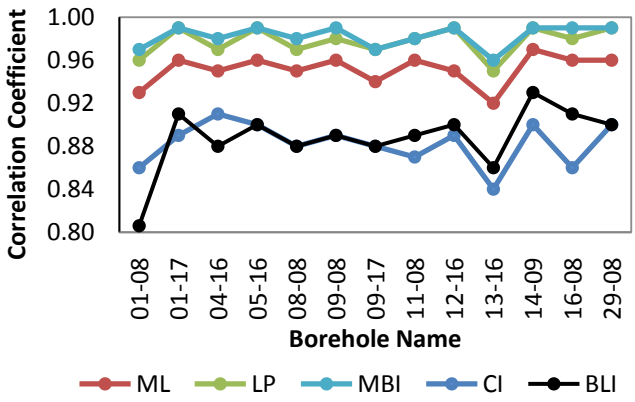

Figure 9: Comparison of correlation coefficient for all inversion methods.

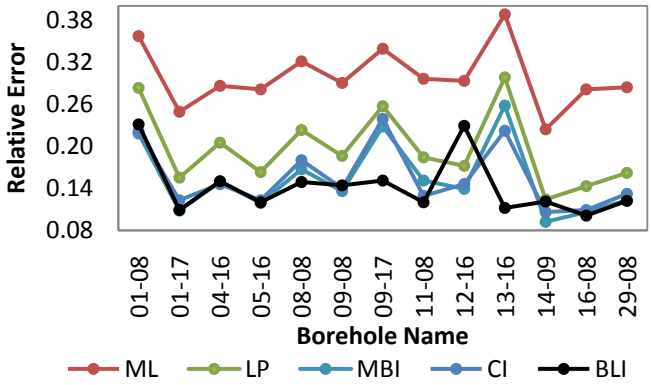

Figure 10: Comparison of Relative Error for all inversion methods.

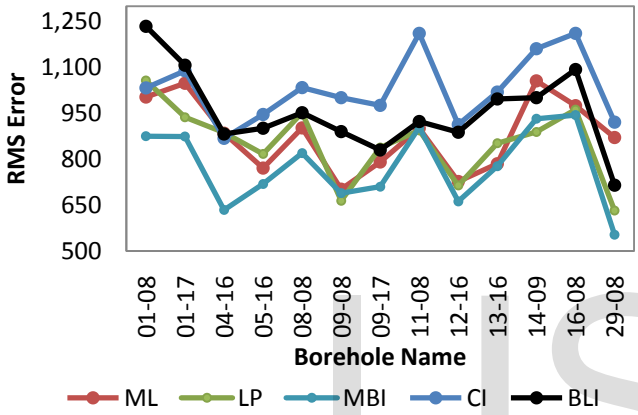

Figure 11: Comparison of RMS Error for all inversion methods.

The average error is 778.6(m/s)*(g/cc). Figure 11 shows comparison of RMS Error for all inversion methods.

A cross section of the inversion result is given in Figure 12. Entire seismic section is inverted into impedance, and shown in this figure for all inversion methods used in this study. Figure 12a is cross-section of inverted impedance using MBI approach. Figure 12b, 12c, 12d and 12e are cross-section of inverted impedance estimated using CI, LPSSI, MLSSI and BLI approach respectively. A low impedances near 1060ms level are clearly visible and highlighted by the rectangle. The low impedance zone is extends nearly 1065ms. This low impedance is may be due to presence of sand channel in this zone. The low impedance zone is seen in all inverted results as it can be seen in figure 12.

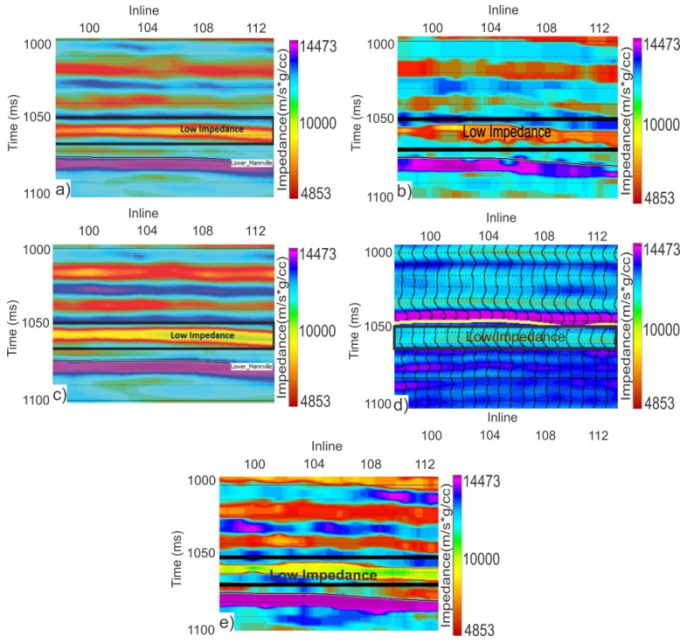

Figure 12: Cross-section of inverted impedance using a) MBI, b) CI, c) LPSSI, d) MLSSI and e) BLI algorithms.

A cross section of the inverted density is given in Figure 13. Figure 13a is cross-section of inverted density using MBI approach. Figure 13b, 13c, 13d and 13e are cross-section of inverted density estimated using CI, LPSSI, MLSSI and BLI approach respectively. A low density near 1060ms level are clearly visible and highlighted by the rectangle. The low density zone is extends nearly 1065ms. This low density zone is may be due to presence of sand channel as it is also seen in impedance section. The low density zone is seen in all inverted results as it can be seen in figure 13.

4.2 Geostatistical Methods

In this section results for the estimation of porosity using seismic attributes are discussed. The prediction is carried out using neural network algorithms. The analysis data is consist of thirteen wells with measured porosity logs, along

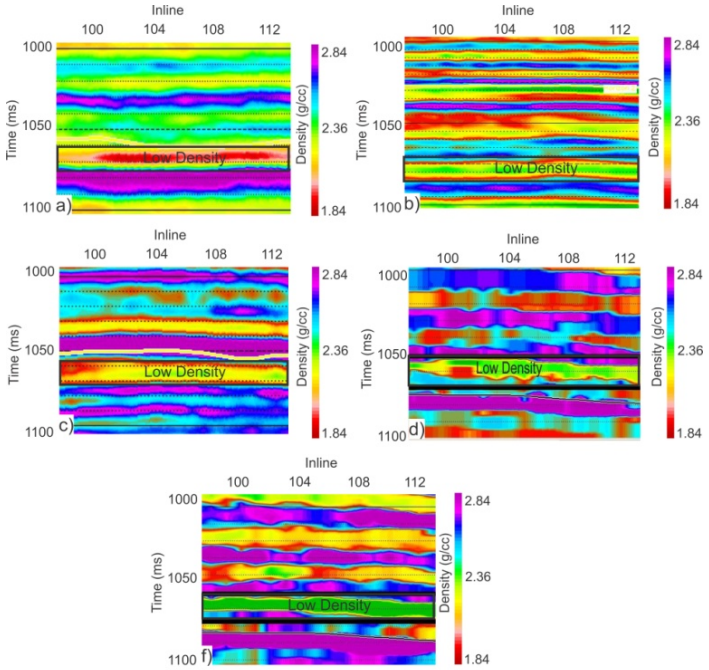

Figure 13: Cross-section of inverted density using a) MBI, b) CI, c) LPSSI, d) MLSSI and e) BLI algorithms.

with the seismic volume and inverted results from the colored, model based and sparse spike inversion methods.

Figures 11a, 11b and 11c show the cross-plot between the predicted porosity and the actual porosity for the colored, the model-based and the sparse spike inversion methods respectively and using probabilistic neural network (PNN) technique as a prediction tool. The y-axis shows predicted density porosity whereas x-axis shows actual porosity from well log data.

The red line is not a regression line in the figures 11a, 11b and 11c but a line with zero intercept and slope 1 which is indicating perfect correlation between predicted and actual attributes. The actual correlation and error are printed at the top , and we can see that the correlation coefficients are 0.81, 0.84 and 0.86 for colored, model based and sparse spike inversion case. The errors are as 3.3306 for colored inversion, 3.408 for model based and 3.271 for sparse spike inversion case.

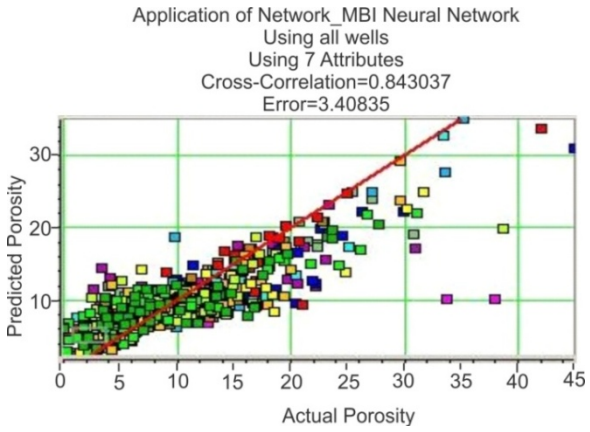

Figure 14: Cross-section of inverted impedance using a) MBI, b) CI, c) LPSSI, d) MLSSI and e) BLI algorithms.

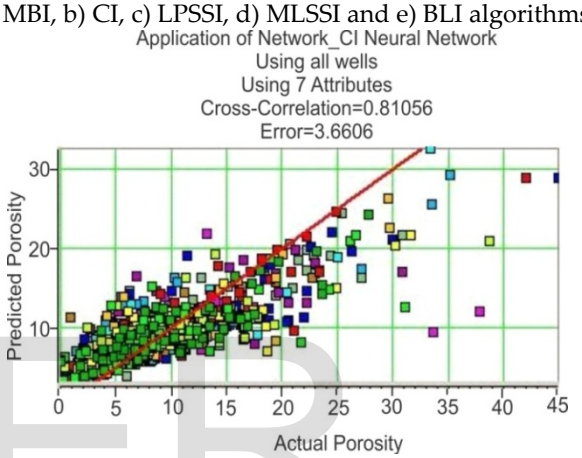

Figure 15: Cross-section of inverted impedance using a) MBI, b) CI, c) LPSSI, d) MLSSI and e) BLI algorithms.

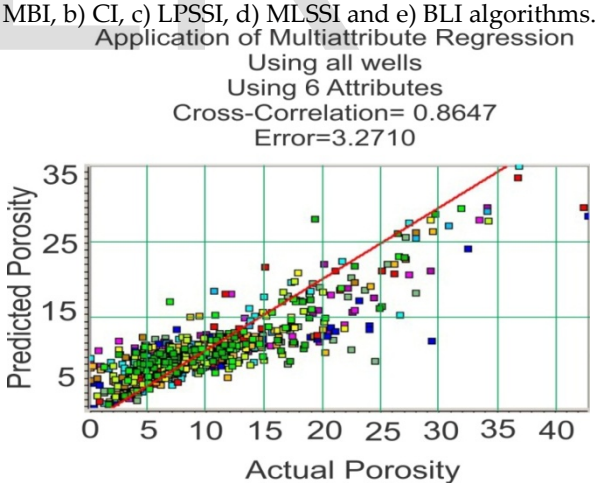

Figure 16: Cross-section of inverted impedance using a) MBI, b) CI, c) LPSSI, d) MLSSI and e) BLI algorithms.

The variation of the predicted porosities when using colored inversion, model based and sparse spike inverted results as external attributes are plotted in Figures 17a, 17b and 17c (shown only xline 41), respectively. The predicted porosity isshown from time 1000ms to 1100ms (only zone of interest). The high porosity zones are interpreted as sand channels (Reservoir).

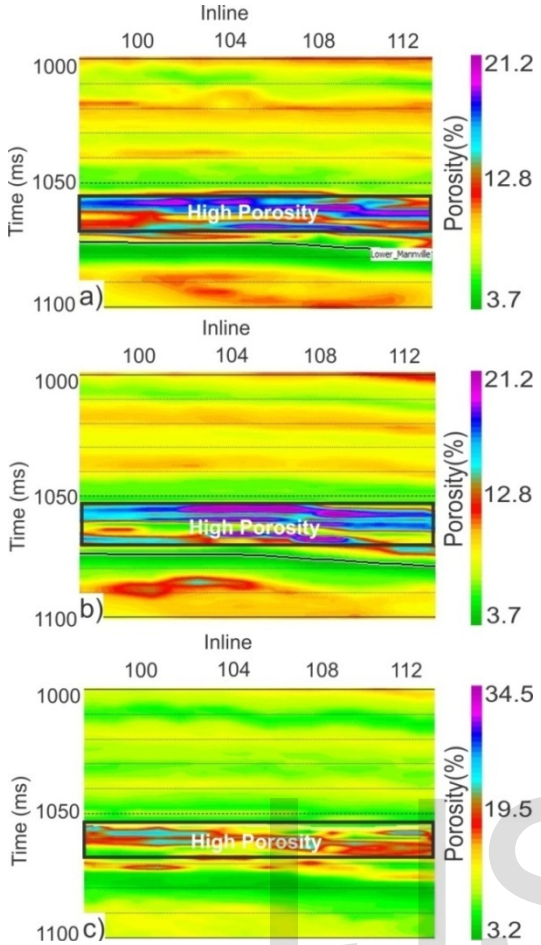

Figure 17: Predicted Porosity using a) CI, b) MBI and c) LPSSI as external attributes.

Using the PNN approach and colored, model based and sparse spike inverted results as external attributes, A high porosity values are estimated, which is located between 1060ms and 1065ms time interval. The maximum porosity is computed in the sand channel is 16% in the case of colored inversion, 18% for model based inversion and it is 32% for sparse spike inversion.

5 DISCUSSIONS

The first group of methods applied to the data is the post-stack acoustic impedance inversion. Four algorithms are used, as described in methodology section. All seismic inversion (model-based, colored, sparse spike and band-limited inversions) results are closely related. These algorithms are tested at the well locations to compare the acoustic impedance inversion inverted results to the log impedance. These seismic inversion techniques estimate similar results, and the tests show reasonable correlation coefficient (0.80-0.99) and RMS average variations, which ranged from 500 (m/s)*(g/cc) to 1300 (m/s)*(g/cc).

The low-impedance zone located between 1060 to 1065ms time levels corresponding to the reservoir. This low impedance zone between 1060ms and 1065ms is also estimated by [15]. The low acoustic impedance varied from 6800 to 8000 (m/s)*(g/cc). The algorithms of the post-stack inversion give similar results, except that in the sparsespike method, where the image appeared is to be more spatially coherent.

Table 1 shows a comparison of results in the reservoir zone between 1060 and 1065ms obtained from all inversion methods. Column 1 (Table 1) is the estimated properties for reservoir zone; column 2 to 6 is the inversion type used in the present study. The table shows that the impedance (6000-6600m/s*g/cc) and density variations (1.8-2.02g/cc) in the reservoir zone are smallest for linear programming sparse spike inversion (LPSSI). The correlation coefficient (0.99) is highest and RMS error (778.36) is least for model-based inversion indicating that the inverted results are most accurately represented subsurface. The cross-correlation (0.86) and predicted porosity (32%) is highest for linear programming sparse spike inversion method when Probabilistic neural network used as prediction tools. This indicates that the linear programming inversion technique is more accurate compared to other techniques for prediction of petrophysical parameters for Blackfoot seismic data.

Table 1: Quantitative comparison of all methods.

Properties	MBI	CI	SSI		BLI
			LP	ML	
Impedance (*10^3)	6.2-7	7-7.5	6-6.6	7.9-8	7-8
Density (g/cc)	1.9-2.4	1.9-2.5	1.8-2	1.9-2	1.8-2
Correlation	0.98	0.89	0.97	0.95	0.92
RMS Error (g/cc*m/s)	778	1029	888	878	963
Relative Error	0.665	0.923	0.206	0.302	0.878
Probabilistic Neural Network					
Cross Correlation	.84	0.81	0.87		
Average Error	3.408	3.661	3.271		
Porosity	18%	16%	32%		

6 CONCLUSIONS

In this study the Blackfoot 3D seismic datasets is used for comparative analysis of several types of post-stack inversion techniques. Extracted a variety of seismic attributes like impedance, density and porosity using these

inversion techniques. The final stacked sections shows good images within the time-depth ranges of 300 to 1300ms, where the target Glauconitic channel is located. From the study it is concluded that:

1. The results shows that model-based, colored, sparse spike and band-limited inversion methods give good and mutually consistent results, with low-impedance zones corresponding to the target hydrocarbon sand within the channel.
2. Probabilistic neural network was utilized to predict the porosity values in this study. Probabilistic neural network show that LPSSI, when used as an external attribute, is more accurate and produces high-resolution images compared to those estimated with the use of MBI and CI as an attribute. From the analyses, the predicted logs showed correlation of 0.81, 0.84 and 0.86 for inversions (CI, MBI and LPSSI) using neural network algorithm as a prediction tool for inversion.
3. The generated porosity cubes show similar high porosity values that correlate well with the low impedance zone.

In an overall conclusion, post-stack inversion produced the best results suitable for provisional targeting gas well. Since this method clearly confirms thereservoir in the channel area. The maximum porosity in the sand channel is 18% when MBI is used as an external attribute; it is 16% in the case of CI and become 32% when LPSSI is used as external attributes. The results suggest that given seismic and well log data for a region, a combination of linear programming sparse spike inversion and PNN can produce a more reliable estimate of the petrophysical properties of the subsurface for the Blackfoot seismic data.

ACKNOWLEDGEMENT

We thank CGG Veritas for providing the HRS software and the Blackfoot seismic data for processing and analyzing and their incessant support for research and development work. We are also grateful to some of our colleagues for the support and fruitful discussions.

REFERENCE

[1]. Berteussen, K. and Ursin, B. (1983). Approximate computation of the acoustic impedance from seismic data. Geophysics, 48(10):1351-1358.
[2]. Chambers, R. L., Zinger, M. L., and Kelly, M. C. (1994). Constraining geostatistical reservoir descriptions with 3-d seismic data to reduce uncertainty.
[3]. Clochard, V., 385 Delepine, N., Labat, K., Ricarte, P., et al. (2009). Post-stack versus pre-stack stratigraphic inversion for co2 monitoring purposes: A case study for the saline aquifer of the sleipner field. In 2009 SEG Annual Meeting. Society of Exploration Geophysicists.
[4]. Downton, J. E. (2005). Seismic parameter estimation from AVO inversion.
[5]. Doyen, P. M. (1988). Porosity from seismic data: A geostatistical approach. Geophysics, 53(10):1263-1275.
[6]. Dufour, J., Squires, J., Goodway, W. N., Edmunds, A., and Shook, I. (2002). Integrated geological and geophysical interpretation case study, and lame rock parameter extractions using avo analysis on the blackfoot 3c-3d seismic data, southern alberta, canada. Geophysics, 67(1):27-37.
[7]. Ferguson, R. J. and Margrave, G. F. (1996). A simple algorithm for band-limited impedance inversion. 395 CREWES annual.
[8]. Haas, A. and Dubrule, O. (1994). Geostatical inversion-a sequential method of stochastic reservoir modelling constrined by seismic data. First break, 12(11).
[9]. Hampson, D. P., Schuelke, J. S., and Quirein, J. A. (2001). Use of multiattribute transforms to predict log properties from seismic data. Geophysics, 66(1):220-236.
[10]. Krebs, J. R., Anderson, J. E., Hinkley, D., Neelamani, R., Lee, S., Baumstein, A., and Lacasse, M.-D.(2009). Fast full-wave field seismic inversion using encoded sources. Geophysics, 74(6):WCC177-WCC188.
[11]. Lancaster, S., Whitcombe, D., et al. (2000). Fast track coloured inversion.
[12]. Latimer, R. B., Davidson, R., and Van Riel, P. (2000). An interpreter's guide to understanding and working with seismic-derived acoustic impedance data. The leading edge, 19(3):242-256.
[13]. Lawton, D., Stewart, R., Cordsen, A., and Hrycak, S. (1996). Design review of the blackfoot 3c-3d seismic program. The CREWES Project Research Report, 8.
[14]. Lindseth, R. O. (1979). Synthetic sonic logs-a process for stratigraphic interpretation. Geophysics, 414 44(1):3-26.
[15]. Mallick, S. (1995). Model-based inversion of amplitude-variations-with-offset data using a genetic 416 algorithm. Geophysics, 60(4):939-954.
[16]. Margrave, G. F., Lawton, D. C., and Stewart, R. R. (1998). Interpreting channel sands with 3c-3d seismic data. The Leading Edge, 17(4):509-513.
[17]. Maurya, S. and Singh, K. (2015b). Reservoir characterization using model based inversion and probabilistic neural network. In 1st international conference on Recent trend in engineering and Technology.
[18]. Maurya, S. P. and Singh, K. (2015a). Band-limited impedance inversion of blackfoot field alberta, canada. In 37th Annual Convention Seminar and Exhibition on Exploration Geophysics.
[19]. Morozov, I. B. and Ma, J. (2009). Accurate poststack acoustic-impedance inversion by well-log calibration. Geophysics, 74(5):R59-R67.
[20]. Neep, J. (2007). Time variant coloured inversion and spectral blueing. In 69th EAGE Conference & Exhibition.
[21]. Pendrel, J. (2006). Seismic inversion-a critical tool in reservoir characterization. Scandinavian oil-gas magazine, 5(6):19{22.
[22]. Russell, B. (1999). Comparison of poststack seismic inversion methods. In SEG Technical Program Expanded Abstracts, number 10.
[23]. Russell, B., Hampson, D., Schuelke, J., and Quirein, J. (1997). Multiattribute seismic analysis. The Leading Edge, 16(10):1439{1444.
[24]. Simin, V., Harrison, M. P., and Lorentz, G. A. (1996). Processing the blackfoot 3c-3d seismic survey. Technical report, CREWES Research Report 8.

[25]. Waters, K. (1987). Reection seismology, a tool for energy resource exploration.